Single Chain Stretching of Block Copolymers under Different Solvent Conditions

Nam-Kyung Lee,[†] Albert Johner,[†,‡] and Thomas A. Vilgis*[,†,‡]

Max Planck Institut for Polymer Research, 10 Ackermannweg, 55128 Mainz, Germany; and Laboratoire Européen Associé, Institut Charles Sadron, 6 rue Boussingault, 67083 Strasbourg Cedex, France

Received December 19, 2001; Revised Manuscript Received March 25, 2002

ABSTRACT: We present a study of the single chain elastic response for block copolymers and multiblock copolymers in selective solvents. The structures of the block copolymers are examples for the richness of single chain force extension relationships. The structure is mainly determined by the interplay of the interactions between the different blocks. Different regimes are discussed: Single micelle contributions, secondary structures, and multimicelle phases. Important contributions stem also from adsorbed bridges between different micelles in a multiblock copolymer.

1. Introduction

Single chain stretching, or atomic force microscopy, has become an important tool in recent years.[1−5] It seems to be an excellent additional technique to study structures of single chains in view of their elastic response. Such a development in experiments allows to detect the interplay between entropy and energy contributions to the chain conformation. The resulting force-extension relations in various polymer systems (including biopolymers like proteins) are rich. In some polymer systems, intrachain self-assembly produces secondary, tertiary structures and the elastic responses manifest these structural hierarchy. Our motivation to study AB diblock copolymers is to provide theoretical understandings of the elasticity of polymer systems, which form different structures depending on the solvent quality for each block. Furthermore, in a selective solvent, a multiblock copolymer forms a secondary structure. Structural transition (unfolding) can be characterized by a force-extension curve.

Indeed single chain stretching has a long tradition in polymer theory. Most of the classical theories of rubber elasticity use models where the elastic behavior of a single chain is studied first, before the calculation of the elastic properties of the macroscopic network.[6−8] For a Gaussian chain the model is very simple: The elastic force is purely entropic and is simply governed by the number of conformations of a chain with fixed ends at a distance R. The number of conformations is given by a Gaussian distribution $P(\mathbf{R}) \propto \exp(-3R^2/(2Nb^2))$. Taking the logarithm yields the corresponding free energy of entropic origin and the resulting force is given by

$$\varphi = \frac{3k_B T}{b}\left(\frac{R}{Nb}\right) \tag{1.1}$$

This is nothing but Hooke's law, but entirely determined by the entropic contribution. The force is proportional to the temperature and the single chain modulus is defined by the mean square end-to-end distance of the chain $\langle R^2\rangle = Nb^2$. This linear regime can be detected in most of the experiments, whenever the energetic contributions to the force are neglected. At larger deformations, $R/b > \sqrt{N}$, the finite chain length has to be taken into account, and the force rises strongly (it diverges theoretically), since less and less conformations are available at large extensions.

In a good solvent, where the chains take self-avoiding walks (SAW), conformations can be treated in a similar way. An instructive model is the construction of "Pincus blobs"[9,10] where it is assumed that a certain force φ corresponds to a typical length scale $\xi_P = k_B T/\varphi$. Inside these at larger forces linearly aligned blobs, the chain possesses still good solvent correlations. It can be shown by simple arguments that the force is no longer linear with the extension

$$\varphi \simeq \frac{k_B T}{b}\left(\frac{R}{Nb}\right)^{3/2} \tag{1.2}$$

Nonlinear response is due to the non-Gaussian scaling of the SAW chain and reflects the asymptotic free energy $F \propto k_B T(R/(N^{3/5}b))^{5/2}$. For larger extensions, the finite chain corrections must be taken into account here as well.

Another interesting case are chains in a poor solvent, where the second virial coefficient v is negative and the chain is stabilized by the repulsive three body interaction.[10,11] The chain collapses to a globular conformation. The monomer concentration $c(\sim \tau/b^3)$ inside of the globule is mainly determined by the balance of the second $(-\tau b^3 c)$ and third virial $(b^6 c^2)$ contribution to the free energy. The parameter $\tau = |T - \Theta|/\Theta$ measures the quality of the poor solvent as the relative distance from the Θ point, where the chains take Gaussian statistics. The size of the chain is then given by $R \simeq b(N/\tau)^{1/3}$ and this result is again interpreted in terms of blobs, the thermal blobs of size $\xi_T = b/\tau$. For all scales smaller than ξ_T, the chain statistics are unperturbed by volume interaction and a chain is a random walk of g_T monomers. On length scales larger than ξ_T, the attraction dominates; therefore the globule can be modeled by a close packing of thermal blobs. The size R of the globule

[†] Max Planck Institut for Polymer Research.
[‡] Institut Charles Sadron.

10.1021/ma012208q CCC: $22.00
Published on Web 06/12/2002

with monomer density c is equal to $R \approx \xi_T(N/g_T)^{1/3} \approx b\tau^{-1/3}N^{1/3}$. The force balance upon pulling the chain out of the globule is then given by $\xi_p = \xi_T$, which leads to[12]

$$\varphi = \frac{k_B T}{b}\tau \tag{1.3}$$

The force corresponds to the natural line tension $\sigma \equiv \varphi = k_B T/\xi_T$ and does not depend on the extension at all. The latter point corresponds to a first-order transition and a coexistence between a certain number of thermal and Pincus blobs.[12]

Another useful example is the elastic response of a pearl necklace structure in polyelectrolytes in poor solvent.[13−15] This more complicated problem can be understood simply in the many pearl regime from the force balance between the electrostatic repulsion of the two half-necklaces and the line tension which connects them.

$$\varphi = k_B T\left(\frac{\tau}{b} - \frac{l_B f^2}{b}\frac{1}{R^2}\right) \tag{1.4}$$

The first term corresponds to the neutral globule properties. Naturally it is the same as in eq 1.3. The second term is the resulting force from the Coulomb repulsion of a chain with charge fraction f (l_B is the Bjerrum length and describes the strength of the Coulomb interaction in terms of temperature, elementary charge, and dielectric constant.)

These three elementary examples show a clear relationship between force, thermodynamic situation, and structure. The AFM technique provides a powerful tool to probe interaction potentials in polymers, or interactions with the environment. These above examples show that blob pictures turn out to be very instructive to get the first feeling of the physics. Nevertheless more refined theories are necessary to support simple predictions based on simple blob pictures.

In the present paper, we are going to study the single chain stretching of a block copolymer in a selective solvent. A diblock copolymer consists of two joined blocks of two chemically different units A and B. The system of block copolymers is useful, because it has been studied already to a great extend. For our purpose the most interesting are the cases, where for one of the blocks the solvent quality is poor, whereas for the other part the solvent is good (or Θ). A number of several situations are imaginable, which are worthwhile to study. The force extension relation of a multiblock copolymer in a selective solvent condition is much richer as we will show below.

2. Stretching a Diblock Copolymer

We consider first a diblock A−B copolymer of total length $L = Nb$ (b is the monomer size) of which the first part of the contour length fL of the copolymer chain consists of the type A and the second part of $(1 - f)L$ of the type B. f is the fraction of A monomers in diblock copolymer, $0 < f < 1$. We discuss the force extension of a diblock copolymer in the case that each part of diblock copolymer is effectively in different solvent condition. When force is applied on one end. The standard

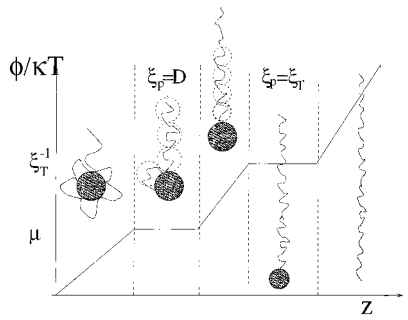

Figure 1. Force extension relation for a diblock copolymer in a selective solvent. The different regimes correspond to the (blob) pictures assigned to each plateau.

Edwards Hamiltonian for such a system under tension is given by

$$\frac{H}{k_B T} = \frac{3}{2b^2}\int_0^{fL} \mathrm{d}s \left(\frac{\partial \mathbf{R}_A}{\partial s}\right)^2 + \frac{3}{2b^2}\int_{fL}^{L} \mathrm{d}s \left(\frac{\partial \mathbf{R}_B}{\partial s}\right)^2 + \frac{v_{AA}}{2!}\int_0^{fL}\int_0^{fL} \mathrm{d}s\, \mathrm{d}s'\, \delta(\mathbf{R}_A(s) - \mathbf{R}_A(s')) + \frac{v_{BB}}{2!}\int_{fL}^{L}\int_{fL}^{L} \mathrm{d}s\, \mathrm{d}s'\, \delta(\mathbf{R}_B(s) - \mathbf{R}_B(s')) + v_{AB}\int_{fL}^{L}\int_0^{fL} \mathrm{d}s\, \mathrm{d}s'\, \delta(\mathbf{R}_A(s) - \mathbf{R}_B(s')) + \frac{w}{3!}\int_0^{L} \mathrm{d}s\, \mathrm{d}s'\, \mathrm{d}s''\, \delta(\mathbf{R}(s) - \mathbf{R}(s'))\delta(\mathbf{R}(s) - \mathbf{R}(s'')) - \int_0^{L} \mathrm{d}s\, \mathbf{f}\cdot\mathbf{R}(s) \tag{2.1}$$

Here, the parameters v_{AA}, v_{AB}, and v_{BB} are corresponding two-body interaction parameters between A−A, A−B, and B−B monomers, respectively. The third virial coefficient w is a constant on the order of b^6 regardless A or B. Its explicit presence in the following calculations has its reason in stabilizing collapsed parts of the chain in selective solvent. The subscript A(B) indicates that the position vector R of a monomer belongs to the A(B) block only. In block copolymers the situation is more complicated than in the homopolymer globule. Nevertheless the Flory mixing parameter $\chi = v_{AB} - {}^1/_2(v_{AA} + v_{BB})$ takes the essential role for the effective pair interactions of the copolymer in a selective solvent. If χ is smaller than $\chi_c(= 2/N$ if $N_A = N_B = N/2)$, A−B phases are mixed, otherwise the A−B phases are segregated. If both phases are assumed to be in good solvent (or high temperature), the A−B short range attraction is less relevant and the elastic response will be simply a linear superposition of A and B part force-extension curves. For mixed phase, $\chi < \chi_c$, and poor solvent conditions for at least one of the blocks ($v_{AA} < 0$ or $v_{BB} < 0$), the elastic response can be estimated in the following two limits. If the poor solvent condition is dominant, the force will remain constant at $\varphi/k_B T = 1/\xi_T$ while the globule unravels to coil in the form of a tadpole[12,16] (see Figure 1). We observed the constant force regime in force-extension curve using a variational method.[17] In dominant mixing condition, the end-to-end distance will increase drastically when force reach to the strength to break A−B interactions.

In the present paper, we focus on the case when the solvent is poor for the A block ($v_{AA} = -b^3\tau_A$) and good or Θ for the B block. If the interaction between the A−B monomers is still repulsive ($v_{AB} > 0$), the physical picture is a combination of Pincus blobs[9] (response of B

block) and Halperin's and Zhulina's picture[12] (response of A block). In a good solvent, the linear response regime is followed by a strong confinement regime characterized by $\varphi \approx k_B T/b(R/Nb)^{3/2}$ [9] where R is the extension of the chain. In the case that the interaction between A−B is attractive ($v_{AB} < 0$) but $\chi > \chi_c$, B block monomers are likely to be adsorbed on the surface of the globule formed by the A block. To characterize this regime by a mechanical force, we assume that one end of the A block is tethered and the force is applied to the other end of the B block. Effectively, the elastic response coming form the B part is similar to the stretching and removing a adsorbed polymer on the spherical surface which is made of A monomers. Previous studies[18] on elastic response of adsorbed chain show that the stretching force results in a phase transition from the adsorbed chain state into the stretched state. Several differences of adsorption on spherical surface from that on the planar surface are pointed out below.

1. Finite size effects by the spherical surface of the globule are important. The surface area made of A block is proportional to $R_A^2 \approx (\rho N_A)^{2/3} \approx b^{8/3}(N_A/|v_{AA}|)^{2/3}$.

2. The adsorbed chain (B block) is under the influence of the attractive interaction $\mu < 0$ with the surface (A block) if the distance z from the surface satisfies the condition $|\mu|\, z \le 1$. The polymers adsorbed onto a planar surface are generally confined to a thickness $D \sim b|\mu|^{-1}$.[10,19] On a curved surface with positive curvature, $\kappa = 1/R_A$, the effective interaction strength is reduced by κ and the adsorption blob size is given by $D^{-1} \sim b|\mu| - \kappa$.

3. The adsorption capacity N^* can be estimated by minimizing the free energy with respect to N with excluded volume interaction.[20] The monomer concentration is $c = N/R_A^2 D$ therefore the free energy of adsorbed chain with interaction strength $|\mu|$ must have the form

$$\frac{F_{ads}}{k_B T} = -\frac{|\mu| N b^2}{D} + \frac{N}{(D/b)^{1/\nu}} + \frac{v_{BB}}{2}\frac{N^2}{D R_A{}^2} + \frac{w}{3!}\frac{N^3}{D^2 R_A{}^4} \tag{2.2}$$

The optimal value of N^* is estimated to be $N^* \sim (|\mu|/v_{BB})R_A^2 b^2$ for good solvent and $N^* \sim w^{-1/2} R_A^2 b$ for Θ solvent.

4. If $N_B > N^*$, some part of the chain remains out of the influence of the attractive surface and follows random walk statistics.[21] The elastic response of this part of the chain is spring like for small extension and $\langle z \rangle \sim (N/g_P)\xi_P = (N_B - N^*)b(\varphi a/k_B T)^{1/(\nu-1)}$ for large extension where Pincus blob ξ_P consists of g_P monomers $\xi_P \approx k_B T/\varphi \sim b g_P{}^{\nu}$.

Our main goal is to compute a force extension relationship for successively increasing extension z. First, we consider the force which will induce the desorption of the B part of chain from the globular surface. For the weak adsorption limit ($D > \xi_T$), it is reasonable to assume that the first part of stretching is from the desorption of the B block from the A block surface.

The free energy of the chain with one end tail (the contour length of the tail is n_t) a distance z apart from the surface will consist of the free energy of the adsorbed part ($N - n_t$) and a tail part (n_t). The adsorption part of the free energy has again two contributions: The free energy cost by confinement and the energy gain by contacts with surface. Let us first ignore excluded volume effects. Then the free energy is

$$\frac{F}{k_B T} = (N - n_t)b^2/D^2 - |\mu|(N - n_t)b^2/D + z^2/n_t b^2 \tag{2.3}$$

Minimizing the free energy with respect to D and n_t gives $D \sim 2|\mu|^{-1}$ and $n_t \sim 2z|\mu|^{-1}$ respectively. The restoring force is

$$\varphi_r = -\partial F/\partial z \sim -|\mu| k_B T \tag{2.4}$$

This force is independent of z while desorption takes place, suggesting that the external force ($\varphi_{ext} = -\varphi_r$) remains constant while pulling (quasi-static pulling). The same result is obtained from the self-consistent field method as described in refs 8 and 22. A more complete form of the partition function is known for an adsorbed polymer[18,23,24]

$$Z(|\mu|b, z/b) = \frac{b}{\sqrt{\pi} R_g}\exp\left(-\frac{z^2}{4R_g{}^2}\right) + \frac{b}{D} Y(|\mu|b, z/b) \tag{2.5}$$

where

$$Y(|\mu|b, z/b) = \exp(|\mu|^2 R_g{}^2 - z|\mu|)\mathrm{erfc}\left(\frac{z}{2R_g} - \left|\mu\right| R_g\right) \tag{2.6}$$

where R_g is the Gaussian radius of gyration, $R_g{}^2 = (1/6)Nb^2$. Using these expressions, we find the external force required to pull the chain for given z to be

$$\begin{aligned}\varphi_{ext} &= -\frac{k_B T}{Z}\frac{\partial Z}{\partial z} \\ &= \frac{z/2R_g{}^2}{1 + \sqrt{\pi}|\mu|\, R_g \exp\left(\frac{z - z_c}{2R_g}\right)^2 \mathrm{erf}\, c\left(\frac{z - z_c}{2R_g}\right)} + |\mu| \\ &\approx \begin{cases} |\mu| & (z < z_c) \\ z/2R_g{}^2 & (z > z_c) \end{cases}\end{aligned}$$

where $z_c = 2|\mu|R_g{}^2$. For small $z < z_c$, the force is $\varphi/k_B T \sim 1/D$ as predicted from mean field calculation. It is shown as a plateau in Figure 1. While the force is constant, adsorption blobs are rearranged into the direction of force but the blob size remains the same. At $z = z_c$, the adsorption blob size should be equal size of Pincus blob size, as it can be seen also from simple scaling estimates. For large $z > z_c$, blobs become smaller and the size is equal to Pincus blob size. When the Pincus blob size reaches the thermal blob size of A phase, the globule consisting of A block start unraveling. We expect a second plateau in the force-extension curve while thermal blob are pulled out of the globule.[12] Combining all regimes, we find a force extension relation as sketched in Figure 1.

3. Multiblock Copolymer in a Selective Solvent

A natural generalization is the extension of these considerations to multiblock copolymers in a selective solvent. In the following we consider a linear multiblock

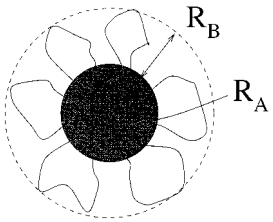

Figure 2. Micelle formation and structure in a multiblock copolymer. The hairy micelle is formed by microphase separation in the selective solvent. The essential structural parameters are given by the radii of the corona and the core.

copolymer consisting of $n_a(=n_b \gg 1)$ AB diblock copolymers joined head to tail. Each diblock copolymer comprises N_A of A monomers and N_B of B monomers so that $N = n_a(N_A + N_B)$. For brevity, we limit our discussion to the asymmetric solvent condition, i.e., we assume $v_{AA} < 0$, $v_{BB} > 0$. Under certain circumstances, a multiblock copolymer forms "hairy" micelles (see also Figure 2) whose cores consist of A monomers and coronas by B monomers. Each micelle consists of p diblocks and there are $n_p = n_a/p$ micelles connected by strings which are also made of B monomers. The optimal size p^* is determined by the interplay of the interfacial energy, the free energy of the core and corona deformation, and the repulsion inside coronas due to the excluded volume effect. Below we use simple geometrical models for the different contributions to the free energies from which we will extract the corresponding elastic response.

A. Noninteracting Micelles. To be more specific, we first consider the case without A−B attractions ($v_{AB} \geq 0$). Under these circumstances the free energy of multiblock copolymer is given by

$$\frac{F}{k_B T} = \frac{4\pi {R_A}^2}{{\xi_T}^2} + p\frac{3}{2}\left(\frac{{R_A}^2}{(N_A/2)b^2} + \frac{{R_B}^2}{(N_B/2)b^2}\right) + \frac{v_B}{2!}\frac{p^2 {N_B}^2}{{R_A}^2 R_B} + \frac{w_B}{3!}\frac{p^3 {N_B}^2}{{R_A}^4 {R_B}^2} \quad (3.1)$$

The free energy terms are described as follows.

1. The first term corresponds to the surface free energy of the core−solvent interface. The surface tension $\gamma = k_B T/\xi_T^2$ is on the order of $k_B T$ per thermal blob at the surface of the globule, which represents the borderline of the core. This term favors the formation of a large micelle, joining all A blocks together.

2. The second and third term correspond to the free energy related to the core and corona deformation in radial direction with respect to their unperturbed dimensions $Nb^2/2$.[25] These terms favor smaller micelles.

3. The last two terms describe the excluded volume effect in good and Θ solvent which are only related to the corona conformation. The monomer concentration in the corona, $c = N_B p/{R_A}^2 R_B$, is used.

The size of each core R_A consisting of p blocks of A monomers is estimated to be $R_A = b(pN_A/\tau)^{1/3}$, in analogy to the poor solvent chain radius. In the case where the B blocks in the corona are ideal chains, they do not interact the associated stretching energy is also negligible. As long as the stretching energy of B blocks (that balances their interaction energy) in eq 3.1 is smaller than the stretching energy of the A blocks, the free energy for the core (the first and second term in eq 3.1) determines the core size. The free energy contribution of a single core made of p blocks is given by in unit of $k_B T$

$$F_{core} = {R_A}^2\tau^2/b^2 + p(2{R_A}^2/N_A b^2) = (pN_A\tau^2)^{2/3} + p(pN_A/\tau)^{2/3}/(N_A b^2) \quad (3.2)$$

The free energy per each core block is then given by

$$\tilde{F} = F_{core}/p = p^{-1/3}(N_A\tau^2)^{2/3} + (pN_A/\tau)^{2/3}/(N_A b^2) \quad (3.3)$$

The minimum is found at

$$p^* = N_A\tau^2/4 \quad (3.4)$$

This suggests that a preferred size of the micelle exists. Each A block will remain as a single core if the reduced temperature satisfies the condition $p^* < 1$, i.e., $\tau < 2/\sqrt{N_A}$, which corresponds to the high-temperature regime. The opposite limit, $p^* > n_a(\tau > 2\sqrt{n_a/N_A})$, corresponds to the case where not enough mass (core block) is available to form an optimal micelle core. In the intermediate temperature regime, more than two core blocks can be formed and structure is rich. This regime will be discussed separately in section 4.1 together with the elastic response of this structure. This result also holds for interacting B blocks provided the interaction energy of the B blocks remains smaller than the stretching energy of the A blocks in the core. For a Θ solvent this is true if the collapsed A block is larger than the Gaussian B block.

At large scales, the conformation of a multiblock copolymer can be viewed as a series of such micelles which carry the optimal number of blocks p^*. Without any attractive interaction between micelles (e.g., exchange of bridges), it is expected that the micelle necklace takes SAW since coronas are repelling each other.

The size of hairy micelle is $R_m = R_A + R_B$, which leads to the span of multiblock copolymer R_{multi} to be

$$R_{multi} \approx R_m(n_a/p^*)^{3/5} \quad (3.5)$$

The corresponding force-extension relation will be of the Pincus type eq 1.2 in a good solvent, when the monomer size b becomes replaced with the micelle size R_m. Therefore

$$\varphi \simeq \frac{k_B T}{R_m}\left(\frac{R}{NR_m}\right)^{3/2} \quad (3.6)$$

This picture holds as long as the Pincus blob size is larger than micelle size, $\xi_P = k_B T/\varphi > R_m$. For large enough force, the micelle necklace will be stretched out.

It can be easily seen that the B blocks start overlapping for $N_B > N_A^{1/3}\tau^{-4/3}$ ($R_B^2 > R_A^2$). Most of the remainder is devoted to the regime where the B blocks do not overlap (and thus not stretch), there our results obviously apply. Other regimes are briefly described in Appendix A for Θ solvent (the good solvent discussion is standard).

B. Interacting Micelles, Phase Diagram. By increasing the attractive interactions between the A and B monomers, new phenomena will occur. It is standard to distinguish several adsorption regimes for increasing B block length or increasing coverage of the micelle core

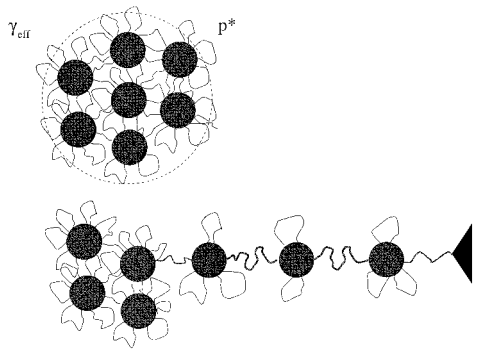

Figure 3. Secondary structure of multiblock copolymers. Under force the chain forms a "pearl necklace structure".

by adsorbed B blocks. One single adsorbed B block can be viewed as a walk of adsorption blobs on the surface of the core made of A blocks. It occupies an area

$$s_B = (N_B(b/D)^{1/\nu})^{2\nu_2}D^2 \tag{3.7}$$

with ν_2 as the relevant swelling exponent in two dimensions ($\nu_2 > \nu$).

If the B blocks overlap, they form a two-dimensional semidilute solution. At higher coverage, the adsorption blobs become dense. This is about how much polymers the adsorption layer can accommodate. For even higher coverage, the excess polymer is stored in a stretched brush structure that completely screens the adsorption layer. Much of the following is devoted to the case where there is on average no extra B block (in addition to the topological one) in the contact area between two micelles R_mD or to the dilute-surface regime.

One important issue is whether the B-polymer can (or cannot) freely enter the contact area. It is commonly admitted that chains do not exchange between the gap and the exterior.[26] In the following, it is implicitly assumed that there is no qualitative change in coverage in the gap. In the following we will mainly consider the case where the adsorbed B blocks do not overlap to the extend to stretch out.

The attractive interaction between the A−B blocks will cause new structures by adsorption of loops and bridges. When $p^* < n_a(= n_b)$, more than two micelle cores are formed and these are combined to each other by bridges (coronas). The connected micelles form a self-assembled globule in a large scale ($N/p^* \gg 1$). The secondary structure in block copolymers is a dense super globule consisting of micelles, which is indicated in Figure 3. The size of the super globule is

$$R_{multi} \sim \left(\frac{n_a}{p^*}\right)^{1/3} R_m \tag{3.8}$$

The cores are connected by adsorbed coronas on the spherical surface of A block polymer. A similar self-assembly structure of micelles is found in a long polysoap where self-assembly is induced due to the amphiphilic monomers on the sequence of the chain.[27] We expect a distinctive elastic response associated with unraveling of this secondary structure. In Figure 4, we show the phase diagram of the multiblock copolymer in $\mu - \tau$ space.

A similar kind of secondary structure may be formed by interconnecting corona blocks between different micelle cores. Then several B blocks connect a pair of adjacent micelles. The entire structure forms then a physical microgel. In the next section, we discuss elastic response of the secondary structure of micelles in detail.

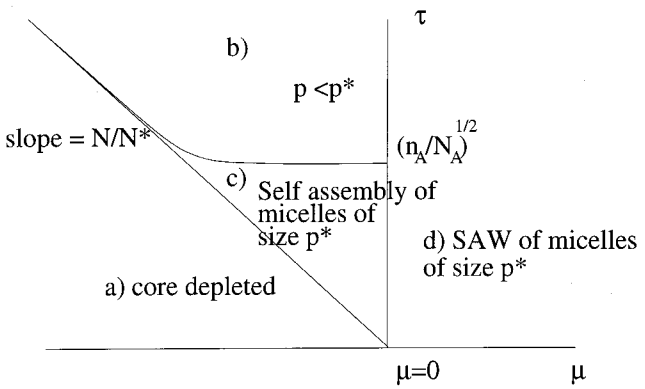

Figure 4. Different conformations of a multiblock copolymer in various solvent conditions and interaction strengths. Microgel phases can be formed in regime c and (d) by exchange of coronas among core blocks.

4. Stretching of Multiblock Copolymers

We showed, in the previous section, section 3, that diverse secondary structures can be formed out of a multiblock copolymer chain. The interesting question is, How does such a structure resolve under external forces? Intuitively it is clear that the first deformation process comes from the deformation of the self-assembly structure (super globule) from sphere to elongated ellipsoid. The force-extension relation is linear in this small deformation. The ellipsoidal deformation of the globule is followed by the dissociation of each micelle aligned on the direction of pulling (see Figure 3). The elastic response of such a super globule of micelles resembles that of the collapsed homopolymer globule[12] in a poor solvent. Following the scenario of the unfolding of a globule, there is a coexistence regime of the aligned micelle structure and the elongated globular structure. This leads to the appearance of van der Waals loop in force-extension curves. As a result, each micelle is detached from the globular structure in a form of tadpole. Upon the onset of unfolding of the secondary structure (if the secondary structure is based on adsorption type bridges), the force remains constant, $\varphi_c = k_BT\mu$, over which the elastic energy exceeds the energy gain by adsorption between micelles. Dissolving the secondary structure is followed by the unfolding of each micelle core (primary structure).

Below, we investigate elastic response of multiblock copolymer micelle-assembly (when there are more than two cores $n_p = n_a/p^* \geq 2$) in more detail. These cores are connected by bridging of coronas: either by adsorption bridges or by exchange of B blocks between cores. Two types of bridges lead to the different elastic responses upon unfolding of secondary structure. First, we consider the case that cores are connected by adsorption of coronas.

A. Breaking Secondary Structure: Adsorption of Coronas between Cores. When external force is applied, the first elastic response of such a structure is due to the deformation of coronas between two cores. If cores are assembled due to the adsorption of the coronas, the elastic response of coronas between two cores can be mapped intuitively to the problem of adsorption of a single chain between two attractive walls. This has been studied theoretically (analytically in refs 28 and 29 and in ref 32 using MC simulation).

1. Adsorption between Two Plates. We assume that the force required to pull thermal blobs from the core is larger than stretching the parts of the chains in the coronas. When an external force is applied, a micelle will be separated from the rest of the cluster through the desorption of the coronas from cores. We consider thus a B block segment of the chain connecting two core globules. The conformation of this segment consists of combination of loops and bridges (see Appendix B). It is easy to see that the major part of the loop contribution comes from the loops of size $D \sim 1/|\mu|$ with loop length $n_l \sim 1/|\mu|^2 b^2$. As long as $z > D$, we can assume that the loop partition function is not considerably changed by the presence of the second surface. Therefore, the contribution of phantom loops $R_l > z > D$ is negligible. We obtain the partition function of a single chain between two attractive wall with separation z as follows:

$$Z(|\mu|, z) = \frac{e^{|\mu|b}}{(z/b - 1)|\mu|b}\left[Y\left(\left|\mu\right|b, \frac{z}{b}\right) - \frac{b}{z}Y\left(\frac{|\mu|b^2}{z}, \frac{z}{b}\right)\right] \tag{4.1}$$

where the function $Y(|\mu|b, z/b)$ is defined in the previous section in eq 2.5.

In strong adsorption limit ($|\mu|z \gg 1$), in addition to loops and bridges, the train contribution becomes important. This regime is discussed in Appendix C.

We propose another solution for the separation z smaller than the radius of gyration of the B-chain. This and the previous solution both apply for $D < z < R_g$ where they trivially match. In a close gap $z < R_g$, the partition function of a chain is dominated by the ground state of the Edwards equation:

$$\frac{\partial Z}{\partial n} = \frac{b^2}{6}\frac{\partial^2 Z}{\partial n^2} \tag{4.2}$$

supplemented by the boundary condition

$$\frac{\partial Z}{\partial z}(\pm z/2) = \pm\frac{1}{D} \tag{4.3}$$

This diffusion equation is easily solved and the detailed solution is shown in Appendix D. Under certain circumstances, the distribution function Z is an equivalent solution of the Edwards equation between two parallel plates, see refs 28 and 29.

For $z < 2D$, we obtain the eigenvalue $\lambda \sim -(k_B T b^2/6zD)$ associated with an even eigenfunction. The corresponding free energy is

$$F_{ads} = \lambda N \sim -k_B T\frac{b^2 N}{6zD} = -k_B T\frac{R_g^2}{zD} \tag{4.4}$$

where the reference is taken at infinite separation. As expected the free energy of adsorption diverges for vanishing gap size. This results in an attractive force between two plates of the order $\varphi_r \sim -k_B T R_g^2/z^2 D$. For $z > 2D$, there is also an odd eigenfunction corresponding to a bound state; this is reminiscent of the compression of the adsorbed chain against a repulsive wall where there is no bridging. The corresponding eigenvalue starts from zero at the threshold $z = 2D$. In the large gap limit ($z \gg 2D$), the eigen values corresponding to the even and odd eigenfunction both saturate at $-(b^2/6D^2)$. In this limit the leading contributions from the even and odd bound eigenstates to the partition function of a chain with one end fixed at each wall almost cancel against each other. The remaining partition function decreases with separation as $\propto\exp(-z/D)$. For separations $z > 2D$, the force is thus independent of the separation and equal to $k_B T/D$.

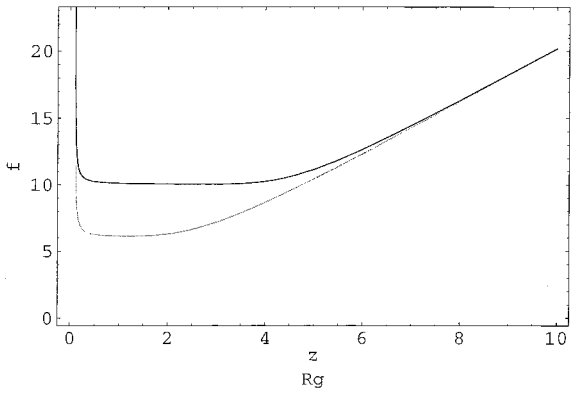

Figure 5. External force as a function of the distance for various interaction strengths $|\mu|R_g = 1, 3, 5$ from bottom to top.

This yields three distinctive regimes for the resulting force between the surfaces.

$$\varphi_{ext}/k_B T \approx \begin{cases} 2R_g^2/z^2 D & (z < 2D) \\ 1/D + 4\dfrac{N}{D^3}\exp(-z/D) & (2D < z < z_c) \\ z/2R_g^2 & (z > z_c) \end{cases}$$

The quantity $z_c = 2R_g^2/D$ describes the extension beyond which the chain elasticity becomes springlike.

The evaluation of force-extension relation from eq 4.5 is shown in Figure 5 for various interaction strengths $|\mu|R_g = 1, 3, 5$. For large extension, it recovers the ideal noninteracting chain behavior. The constant force regime increases as the interaction strength becomes larger. At large surface separations, the number of bridges becomes unity and we recover the single surface adsorption solution.

The divergence of the attractive interaction between two plates at monomer size is an obvious artifact of ideal chain approximation. When two surfaces are strongly close to each other for $z \leq 2D$, the loops size is limited by the second surface. The phantom loops $R_l > z$ contribution to the partition sum must be subtracted. We tried to correct for that by using the standard eigenmode decomposition.

Loops (as opposed to topological bridges) also adsorb on the micelle core and may bridge between two micelles. It is easy to deduce the partition function of an adsorbed polymer with both ends on the same plate as a function of the separation from the eigenstates. For large gaps, $z > 2D$, the even and odd eigenstate contributions have the same sign and the single plate result is asymptotically recovered. For close gaps, $z < 2D$, the eigenfunction is even and the free energy is the same as for the a chain with one end on each plate (bridge) at the level of the ground-state approximation. In closer gaps ($z \ll 2D$), the precise location of the ends is (almost) irrelevant.

A more important correction, however, is given by the excluded volume effect. In Θ solvent condition $v_2 = 0$, the excluded volume term is given by third virial term $\delta F_w = w/3!\phi^3\delta V$. The third virial contribution to the

monomer chemical potential $wf^2/2$ remains perturbative to the eigenvalues at large separation. The repulsive correction to the eigenvalue of the even bound state is obtained by averaging over the unperturbed eigenstate.[33] In the perturbation scheme, the even bound state is suppressed (the eigenvalue becomes positive) for $z < D$ where $w \sim b^6$ is assumed.[34] There is thus an equilibrium separation between the plates of about D. The decrease of the free energy in the optimal gap with respect to large separations is on the order of $\sim k_B T R_g^2/D^2$ per chain.

As already discussed, attraction of more B-chains into the gap upon micelle−micelle approach is not anticipated. The opposite limit of free B blocks is discussed in the Appendix E.

2. Deformation. We assume a constant number of B blocks per unit core area. The micelles are at equilibrium distance therefore the separation between core surfaces are about D. Using the Derjaguin approximation[30,31] the spring constant for the bridging contact is

$$k_{mD} = k_B T \sigma_{eff} R_m / D^3 \tag{4.5}$$

where σ_{eff} is the fraction of the core surface covered by adsorbed polymer. The free energy of debridging is

$$F^* = -k_B T \sigma_{eff} R_m / D \tag{4.6}$$

Not regularizing the adsorption energy between plates by the third virial term would have produced an additional log D/b factor.

On scales larger than a micelle, the micelle assembly glued by the adsorbing B blocks may be viewed as a dense superglobule micelle located at the external surface lake neighbors and miss the corresponding bridging attraction. This gives rise to an effective surface tension of the super globule

$$\gamma_{eff} = F^*/R_m^2 \tag{4.7}$$

The critical force for unraveling the superglobule is thus, following Halperin and Zhulina,[12] $\varphi_c = k_B T \sigma_{eff}/D$. After unraveling, the string of micelles can be extended according to the spring constant k_{mD}. After this linear regime, adsorbed bridges will relax at the critical force $\varphi_c \sim F^*/D$. The constant force regime $\varphi_c = k_B T/D$ could be seen under imposed elongation.

The extension of the secondary structure under the external force is therefore characterized by two regimes after the initial ellipsoidal deformation. The early corona deformation (related to the corona desorption) gives constant force plateau in force extension curve. The further stretching of string requires the corresponding increase in force and the response is linear.

B. Breaking Secondary Structure: Topological Bridges. A similar kind of secondary structure may form by exchange of corona blocks between two micelle cores: a micelle is visited by the multiblock copolymer more than once. Several B blocks connect a pair of adjacent micelles.

Let us first consider the case of two consecutive micelles along the chemical sequence or, to be specific, the somewhat academic case where only two (optimal) micelles form. For large enough (interacting) B blocks, adsorption takes place only in the blobs closest to the core. The B blocks in the corona stretch out, the correlation length is thus reduced. The outermost blob size gives the largest correlation length in the corona d_{fl}. If the triblock copolymer micelles are brought into classical contact (with an overlap of about d_{fl}), bridging is only driven by small corrections of order $k_B T$ to the free energy. Therefore, of order one bridge forms per outermost blob in the overlap region. Consider the equivalent micelle where all B loops on an isolated p^* micelle are cut into two open chain arms and all A blocks are cut at the central monomer. On this equivalent micelle of telechelic triblock copolymers,[35] on average, one chain end can be found per outermost corona blob. Furthermore, bridging is only driven by small corrections to the free energy. Therefore, a finite fraction of the fictitious end points in the outer edge of the equivalent micelles correspond to bridges. In the multiblock system, the A blocks have to be connected, and this can be done in several ways. The corresponding entropy on the order of the thermal energy per bridge (logarithms are considered to be of order unity at this level of argument) is part of the driving force for bridging introduced previously. The surface density of bridges each of which decrease the free energy by about $k_B T$, is thus $1/d_{fl}^2$. The overlap area of two micelles in classical contact is $\sim R_m d_{fl}$ and the total bridging energy is

$$F_t^* = -k_B T R_m / d_{fl} \tag{4.8}$$

This is relevant provided $R_m > d_{fl}$. It can be understood as the free energy penalty for converting all the bridges on a micelle (but the topological one) into loops.

Under the action of an external force, the micelle separation slightly increases. The spring constant of the micelle−micelle contact in the linear regime (extension by less than d_{fl}) is F^*/d_{fl}^2. The next step would be to increase the micelle separation by several d_{fl}, to release all bridges but one. The critical force to debridge a pair of micelles F^*/d_{fl} is less than the extraction force $k_B T \tau/b$ of A blocks summed over the bridges, but it is typically larger than the extraction force of the last topological bridge.

When there are more than two micelles in the string, micelles that are not topological neighbors may also stick due to bridging attraction. The resulting micellar network is connected by bridges and forms a physical microgel.[35] This happens even when A−B interactions are repulsive. Under external stress such a gel flows. However, to rearrange the micelles they have to overcome some energy barriers and flow only occurs after some waiting time (the connectivity can be complicated in such a gel). This is in principle irrelevant for quasistatic pulling as considered here. However it may become important in real experiments. If the microgel is deformed very slowly, it can flow as an ordinary liquid. However micelles at the gel border have less neighboring micelles this results in an effective surface tension for the microgel

$$\gamma_{gel} = -F_t^*/R_m^2 \tag{4.9}$$

It should be noted that γ_{gel} is small compared to γ_{eff} (eq 4.7) as micelle stability requires at least that the tricritical blob in the A-phase be smaller than the B blobs closest to the core.

As in the classical work by Halperin and Zhulina on unfolding a polymer globule cited above, a much larger force is required to deform the multiblock microgel than

to unwind it in a string of simply connected micelles. The corresponding critical force is

$$\varphi_{cr,m} = k_B T/d_{fl} \tag{4.10}$$

and it is much smaller than both the force $k_B T\tau/b$ for extracting an A block and the force to rupture micelle−micelle contact. When the B blocks are only marginally stretched in the corona the micelle extraction force becomes as weak as $\varphi_{cr,m} \sim k_B T/R_B$, whereas the debridging force becomes on the order of the force to extract the A blocks involved in all bridges.

The analysis of bridging remains rather crude and at the present level benefits a lot from the solution of the simpler case of telechelics.[35] Many metastable states expected should play an important role beyond the somewhat academic quasi-static limit. This requires a more careful study.

C. Breaking the Primary Structure. In this final section, we discuss the breaking of the primary structure, i.e., the dissolution of each micelle. We consider the elastic response of the chain after the external force unfolds all existing cores in the given direction. This also includes the case $p^* < n_a$, so that single micelle is formed out of a multiblock copolymer. Further stretching can be achieved by dissolving cores of preferred size p^*. This procedure also rearranges the blocks which belong to the corona into string. If the force is imposed, the breaks of the core occurs only when the force reaches $k_B T\tau/b$. This force is large enough to dissolve all structures into a series of Pincus blobs. In the case of fairly strong adsorption the force for breaking the adsorption contact may be stronger.

It is more interesting to consider the case when the extension is imposed. Under the tension, releasing a core block out of the optimal size of micelle will reduce the elastic energy. Since the structure of multiblock copolymer is discrete repetition of two different component, the elastic response is discontinuous. The free energy of a multiblock copolymer with n_p aligned micelles which consisting of p^*-core block is given by

$$\frac{F}{k_B T} = n_p \frac{F_{micelle}}{k_B T} = n_p \left[(p^* N_A \tau^2)^{2/3} + p^* \frac{(p^* N_A/\tau)^{2/3}}{N_A b^2} \right] + (n_p - 1)\frac{(z/n_p - 1)^2}{N_B b^2} \tag{4.11}$$

where n_p is the number of micelles $n_p = n_b/p^*$. The last term imposes z as the end-to-end distance. The strings which connect two different micelles contribute the elastic part of the free energy, and there are $n_p - 1$ such strings. Since there is a preferred size p^*, all micelles have about the same size. We neglect the adsorption of B block coronas and the entropy part of coronas as well. Applied tension shifts the optimal sizes of core and corona to smaller size. Such a change in conformation should minimize the surface free energy. A set of A block and B block is separated out from the globule of micelle of p^* blocks. Each release of core block brings a corona block to align in the direction of force. The discreteness of the number of core blocks introduce the nonmonotonic effect in force-extension relation. For a larger extension, it is energetically more favorable to release all core

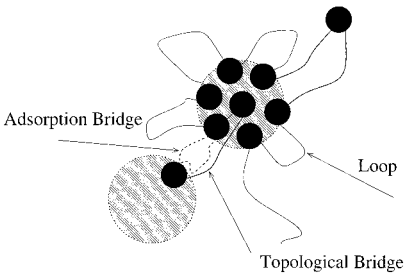

Figure 6. Micelle assembly formed from two different types of bridging attractions: adsorption and topological exchange of coronas between cores.

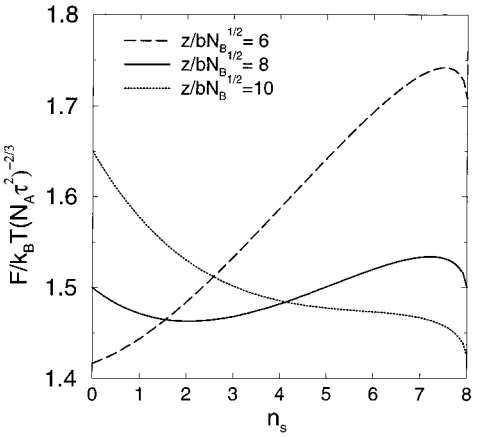

Figure 7. Free energy of a partly extended micelle of which optimal size $p^* = 8$ without external force. The minimum in each curve corresponds to the number of the released core blocks at given extension in the unit of bN_B^2. The optimal value of n_s abruptly increases due to the discreteness of the number of blocks.

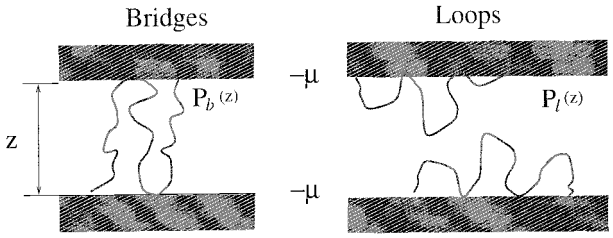

Figure 8. Bridging and looping of polymers between surfaces. The multimicelle problem can be mapped on these structures to find the essential features of the external force.

blocks from a micelle. When n_s core blocks are released from a micelle ($p^* - n_s \ll p^*$), neglecting the core deformation term, the total free energy of the multiblock copolymer with partly dissolved core is

$$\frac{F}{k_B T} = (n_p - 1)\frac{F_{micelle}}{k_B T} + ((p^* - n_s)^{2/3} + n_s)(N_A \tau^2)^{2/3} + \frac{z^2}{(n_p - 1 + n_s)N_B b^2} \tag{4.12}$$

In Figure 7 , we show the free energy of such a micelle for various extensions z (in the unit of $z/b\sqrt{N_B}$) for a system with $p^* = 8$ and $n_p = 8$. For $z < 6$ the minimum is found at $n_s = 0$ implying that all core blocks still belong to a micelle core. For $z = 8$ minimum in free energy curve appears at $n_s = 2$. For larger extensions, $z = 10$, the minimum abruptly shifted to $n_s = p^* = 8$ implying that all the cores are released. The unwinding

of a micelle core is therefore manifested in force extension curve in the following way.

1. After unfolding the first block from micelle core, the force will drop to a small value due to the abrupt release of the attached corona. The repetition of this process will create a sawtooth pattern in the force extension curve.

2. The further stretching drives the remaining micelle core unstable and leads to the abrupt release to open chain configuration. This yields a strong decrease in the force-extension curve.

In the system of many micelles, while one micelle is completely dissolved the others still remain as the preferred size. The unfolding of each micelle will repeat again the above processes 1 and 2.

At the final step stage, all the cores consisting of a single A block can also be unfolded, thus again returning to Halperin and Zhulina's tadpole picture.[12]

5. Conclusion

We discussed the stretching behavior of a regular multiblock A−B copolymer in selective solvent (good for B, poor for A) under the influence of an external force. The predicted force-extension curves reflect the hierarchy of structures (secondary, primary) somewhat similar to that encountered in proteins. In many respects, our approach is based on previous work on diblock or triblock copolymers.

It is known that diblock or triblock copolymers in selective solvents self-assemble to protect the less soluble blocks from contacts with the solvent. The regular multiblock copolymer may be looked at as a polymer of triblocks with a soluble central block and insoluble terminal blocks. Those triblocks form flower micelles where the insoluble blocks form an insoluble core whereas the soluble blocks dangle in the solvent and build the corona. If they are large enough, soluble blocks stretch away from the core and form a brushy layer. For polymeric surfactants (high molecular weight blocks) as considered here, the micelles have a well-defined aggregation number p^* and radius R_m. When a single long multibblock copolymer is put in a selective solvent, similar (intrachain) p^* micelles form that are connected by the polymer backbone.

In addition to this primary structure a secondary structure may be induced by micelle−micelle attraction. We considered explicitly two possible mechanisms that could cause attraction: adsorption of corona blocks onto the cores and related bridging interactions (only expected for shorter soluble blocks); exchange of insoluble blocks between micelles that creates bridges between micelles in addition to those implied by connectivity. The associated multiblock resembles a (physical) microgel. At low frequency, such a physical microgel flows like a liquid, and such a behavior is assumed throughout as we restrict ourselves to the quasi-static limit. We consider the polymer as a superglobule composed of micelles rather than of individual monomers.

Micelles located at the superglobule−solvent interface are lacking favorable interactions with neighboring micelles, and this entails an effective surface tension γ_{eff}. The mechanical properties of the superglobule are very similar to those of an ordinary collapsed globule studied by Halperin and Zhulina. Strongly asymmetric globule shapes are not anticipated, there is a critical force $k_BT/R_m\gamma_{eff}$ for unwinding the superglobule in a string of micelles. This string is almost fully stretched. The elasticity of the micelle−micelle contact determines the behavior of the string of micelles. Rupturing the micelle−micelle contact requires a force that may in certain cases allow for total micelle unwinding.

We hope our calculation to show that force−strain relations on complex single molecules that could be measured in an AFM experiment give some insight into the actual hierarchy of structures. Moreover, more detailed variational principles (beyond scaling) allow for several generalizations in future works. Its technical implementation for polyelectrolytes and polyampholytes is more or less straightforward. However interesting results can be expected depending also on the range of the electrostatic interactions when salt is added. Stress strain relations of random copolymers and polyampholytes[37] offer new insight in the function of these systems which depend on the sequences. These considerations are left for forthcoming papers.

Our treatment of multiblocks remains crude in some respects. Multiblocks may assume more complex connectivity than considered here. We also expect metastable states involving frustrated micelles and complex connectivity to play a role beyond the quasi-static limit. This remains a rather challenging issue.

Acknowledgment. This work was partially supported by a grant from the D.F.G. on polyelectrolytes (N.L.). A.J. and T.A.V. acknowledge the grateful support of the L.E.A.

Appendix A: Optimal Micelle Size with Overlapping Coronas

Depending on the B-block length or increasing coverage of the micelle core, the corona part of free energy contributes the determination of the optimal size of micelles. In this appendix, we consider micelles where the corona can be approximated as flat brushes (crew cut regime) or curved brushes (starlike regime).

First we consider short enough B blocks for the curvature to be negligible in the B-shell ($R_A \gg R_B$), the so-called crew cut micelle regime. The extension R_B of the B blocks is then given by the flat brush height

$$R_B = (w/b^6)^{1/4} N_B (pb^2/R_A^2)^{1/2} b \qquad \text{(A1)}$$

in Θ solvent. This can be qualitatively obtained by the standard Alexander argument under Gaussian statistics. The free energy of the corona is found to be negligible provided the collapsed A-block radius is lager than the Gaussian B-block radius. It is easily checked that this is located in the crew cut (brushy) micelle regime.

For larger B blocks the stretching energy of the B blocks limits the size of the micelle. The optimal aggregation number becomes

$$p^*_{crew-cut} = N_A^2 \tau / N_B^{3/2} \qquad \text{(A2)}$$

The core radius R_A becomes $R_A = N_A/N_B^{1/2} b$ independent of τ. The B-block extension $R_B = N_B^{3/4} \tau^{1/2} b$ becomes independent of N_A. The crossover to the star micelle occurs at $R_B = R_A$, meaning

$$N_B > N_A^{2/3}/\tau^{2/5} \qquad \text{(A3)}$$

Let R_B be the radius of the starlike micelle, the curvature can still be neglected in the outer part of the

corona beyond $R_B/2$. There the flat brush formula can still be used and $R_B = N_B(p/R_B^2)^{1/2}$, implying $R_B = N^{1/2}p^{1/4}$. At the scaling level a fair estimate of the free energy stored in the corona is given by the stretching energy of the B blocks $F_B = k_BTp^{3/2}$.[35] The leading terms in the free energy are now the surface tension between the core and the solvent and the energy in the starlike corona. We obtain

$$p^*_{star} = (N_A\tau^2)^{4/5} \tag{A4}$$

and the corresponding micelle size

$$R_m \sim R_B = N_B{}^{1/2}(N_A\tau^2)^{1/5} \tag{A5}$$

The correlation length (blobsize) d_{fl} at the outer edge of a flat brush in Θ solvent is given by $d_{fl} = N_B^{1/3}(\sigma b^2)^{-1/6}b$ in terms of grafting density σ. It can be recovered from the scaling form of the molecular potential $U(\zeta) = \sigma b^2\zeta/h$ near the brush edge, where ζ is a distance from the classical brush end (i.e the end found when fluctuations are neglected) and h is the height of the brush. We ask for the interaction energy cumulated over the last correlation length to be k_BT. This defines d_{fl} through $\int_0^{d_{fl}} d\zeta^2\sigma\zeta/h = 1$ in agreement with the announced result. As already discussed, in the outer part of the corona curvature is never relevant and the grafting density σ in the previous formula is to be replaced by $\sigma = p^*/R_m{}^2$ and R_m the actual micelle radius ($R_m \approx R_A$ in the crew cut micelle regime, $R_m \approx R_B$ in the star micelle regime). We obtain

$$d_{fl} = \begin{cases} N_B{}^{1/3}\, N_A{}^{1/18}\tau^{-2/9}b & (N_A{}^{1/3}\tau^{-4/3} < N_B < N_A{}^{2/3}\tau^{-2/3}) \\ N_B{}^{5/12}\,\tau^{-1/6}b & (N_A{}^{2/3}\,\tau^{-2/3} < N_B < N_A{}^{4/5}/\tau^{2/5}) \\ N_B{}^{1/2}\, N_A{}^{-1/15}\tau^{-2/15}b & (N_A{}^{4/5}/\tau^{2/5} < N_B) \end{cases}$$

Appendix B: Calculation of Single Chain Partition Function between Two Plates: Loops and Tails

A B-block segment between cores can be considered as a chain tethered the ends to both surfaces (which represent the cores). We assume that there exists at least one bridge because of the connectivity since this is part of a linear chain. We assume further, that the distance between the surfaces z is given. The partition function of a single chain between two attractive walls with separation z can be obtained by estimating the statistical weight of loops and bridges. The probability to form a bridge is given by finding an end at the other surface at distance z. The answer to this question is related to the corresponding first passage problem[36] in the theory of random walks. The probability to form such a bridge is given by

$$p_b(n_b, z) = \frac{z}{n_b b/6}\left(\frac{3}{2\pi n_b b^2}\right)^{1/2} e^{-3z^2/2n_b b^2} \tag{B1}$$

The probability to form a loop (attached to a single surface) is when $z = b$

$$p_l(n_l, z = b) = \frac{1}{n_l/6}\left(\frac{3}{2\pi n_l b^2}\right)^{1/2} e^{-3/2n_l} \tag{B2}$$

Note that each contact with the surface is associated a statistical weight $e^{-\mu b}$. For weak adsorption, $|\mu| < 1$, the partition function of the chain includes all possible combination of loops and bridges:

$$Z(|\mu|b, N, z/b) = \sum_k\sum_k e^{k\mu b}e^{k'|\mu|b}\int p_l(n_1)\ldots p_l(n_k)p_b(m_1)\ldots p_b(m_{k'})\,\delta(N - \sum n_k - \sum m_{k'})dn_1\ldots dn_{k_{max}}\,dm_1\ldots dm_{k'_{max}} \tag{B3}$$

where k and k' are the number of contacts with the surface associated with loops and bridges, respectively. The Laplace transformation allows to decouple the loop and bridge contributions. With $\tilde{p}_l(s) = e^{-\sqrt{s}}\tilde{p}_b(s) = e^{-(z/a)\sqrt{s}}$, we find for the partition function

$$\tilde{Z}(|\mu|b, s, z/b) = \sum_{k_l}\sum_{k_b=1}(\tilde{p}_b(s))^{k_b}(\tilde{p}_l(s))^{k_l}e^{(k_l+k_b)|\mu|b} \approx \frac{e^{-(z/b)\sqrt{s}}e^{|\mu|b}}{\left(\frac{z}{b}\sqrt{s} - \left|\mu\right|b\right)}\frac{1}{(\sqrt{s} - |\mu|b)} \tag{B4}$$

The partition function (eq B4) is the product of the loop and bridge contributions. After inverse Laplace transformation, we obtain the desired results as eq 2.5.

Appendix C: Strong Adsorption Limit

For strong adsorption limit, the partition sum should include "trains". Assuming that the chain to be ideal, the partition function can then be casted in the following form

$$Z_s(N) = \int dN_1\, e^{|\mu|(N-N_1)}Z_1(N_1) = \frac{e^{|\mu|N - z\sqrt{|\mu|}}}{z\sqrt{|\mu|}}\left(\frac{1}{\sqrt{|\mu|} - |\mu|} - \frac{1}{z(\sqrt{|\mu|} - |\mu|/z)}\right) \tag{C1}$$

where Z_1 is the partition sum with bridges and loops consisting of N_1 monomers (see eq 4.1). There are $N - N_1$ monomers belong to trains which provide the weight $e^{|\mu|(N-N_1)}$. The last equality is obtained by performing Laplace transform with respect to μ. The external force required to separate two surfaces is

$$\varphi_{ext} \sim \sqrt{|\mu|} + 1/z + \left(\frac{1}{z^2(\sqrt{|\mu|} - |\mu|/z)} + \frac{1}{z^3(\sqrt{|\mu|} - |\mu|/z)^2}\right)\left(\frac{1}{\sqrt{|\mu|} - |\mu|} - \frac{1}{z(\sqrt{|\mu|} - |\mu|/z)}\right)^{-1} \tag{C2}$$

Note that required force is diverging for very short length scales, i.e., $z = \sqrt{|\mu|}$.

Appendix D: Calculation of Partition Function: Solution of Edward Equations

For convenience we set $b^2/6 = 1$. The Edwards equation is solved by the eigenfunction expansion $\sum_i\psi_i(z_1)\psi_i(z_2)\exp(-\epsilon_i n)$ where index i describes all the eigenfunctions $\psi_i(z)$ of the operator $-\Delta$ and the ϵ_i are the associated eigenvalues. The normalized eigenfunctions are to be calculated with the relevant boundary conditions

$$\frac{d\psi}{\psi\, dz}(\pm z/2) = \pm 1/D \tag{D1}$$

By symmetry, we look for even or odd eigenfunctions. For large chains, the expansion is dominated by bound states (with negative eigenvalues). There is always an even bound state (not yet normalized): $\psi^e(z) = \cosh \sqrt{-\epsilon_e} z$. For $h > 2D$ there is also an odd bound state (not yet normalized): $\psi^o(z) = \sinh \sqrt{-\epsilon_o} z$. The partition function $Z^b(-z/2, z/2)$ for a chain with an end on each plate can be approximated by the bound states contribution, i.e., the "bridge partition function"

$$Z^b(-z/2, z/2) = \begin{cases} \dfrac{\cosh^2 \alpha_e}{I_e} \exp 4N\alpha_e^2/z^2 & (z < 2D) \\ \dfrac{\cosh^2 \alpha_e}{I_e} \exp 4N\alpha_e^2/z^2 - \dfrac{\sinh^2 \alpha_o}{I_o} \exp 4N\alpha_o^2/z^2 & (z > 2D) \end{cases}$$

where $\alpha_e = \sqrt{-\epsilon_e} z/2$ is the solution of $\coth(u) = u2D/z$ and $\alpha_o = \sqrt{-\epsilon_o} z/2$ is the solution of $\tanh(u) = u2D/z$. The crossover to the constant force regime corresponds to large separation where $\alpha_e = \alpha_o = z/D$. The leading factor in eq D2b is then the normalization factor $1/I_{e,o}$ proportional to $\exp(-z/D)$. When both chain ends are fixed on the same plate, the "loop partition function" $Z^l(-z/2, z/2)$ reads

$$Z^l(-z/2, z/2) = \begin{cases} \dfrac{\cosh^2 \alpha_e}{I_e} \exp 4N\alpha_e^2/z^2 & (z < 2D) \\ \dfrac{\cosh^2 \alpha_e}{I_e} \exp 4N\alpha_e^2/z^2 - \dfrac{\sinh^2 \alpha_o}{I_o} \exp 4N\alpha_o^2/z^2 & (z > 2D) \end{cases}$$

For large separations ($z/D \rightarrow \infty$), the single plate partition function is recovered.

Appendix E: Freely Moving B Blocks

In case the B blocks can freely move on the core, the polymer amount in the gap can adjust the separation. Here it is assumed that the layer in the gap is always continuous. For our purpose it is enough to consider close gaps ($z < 2D$) where the concentration ϕ is almost uniform. We will address successively marginal solvent and Θ solvent. Quite generally we may write the free energy per unit area:

$$F/k_BT = -\phi b^2/D + v_2/2\phi^2 z + w/3!\phi^3 z \qquad \text{(E1)}$$

After minimization with respect to ϕ we obtain the concentration as a function of the gap size and the free energy.

In the marginal solvent case $w = 0$, $v_2 > 0$, we find $\phi = b^2/zDv_2$. This means that for close gaps the monomer content is independent of the gap size at this level of arguments, this gives some generality to the obtained results. The equilibrium pressure between flat plates is attractive and given by the pressure in the mid plan and is proportional to $-1/z^2$. Using again the Derjaguin approximation

$$F^* = \frac{b^4 R_m \log D/b}{2D^2 v_2} \qquad \text{(E2)}$$

This result does not show the expected scaling form $\sim (R_m/D)^x$. The mix of the dimension dependent Derjaguin approximation and dimension independent mean-field considerations obscures the picture (the academic use of the four dimensional Derjaguin approximation restores the expected simplicity). In the calculation we took only into account close gaps. The large gap contribution ($z > D$) is dominated by the lower boundary and gives a similar contribution as it has to be (here up to logarithmic corrections).

In the tricritical regime, the second virial is negligible in front of the third one. Following general arguments, the pressure at large gaps ($D < z$) decays as $-k_BT/z^3$. The free energy of interaction between plates is $-k_BT/z^2$ per unit area. Under the Derjaguin approximation we obtain

$$F^* = -k_BTR_m/D \qquad \text{(E3)}$$

where the integral of the force between micelles has been carried out over the outer region (which is enough for the scaling behavior). Note that this result merges with the dilute surface regime for $\sigma_{eff} = 1$. In contrast to the marginal solvent case, the amount of polymer in the gap vanishes for close gaps.

References and Notes

(1) Senden, T. J.; diMeglio, J. M.; Auroy, P. *Eur. Phys. J. B* **1998**, *3*, 211.
(2) Li, H. B.; Rief, M.; Oesterhelt, F.; Gaub, H. E. *Adv. Mater.* **1998**, *10*, 316.
(3) Courvoisier, A.; Isel, F.; François, J.; Maaloum, J. *Langmuir* **1998**, *14*, 3727.
(4) Lee, G. U.; Chrisey, L. A.; Colton, R. J. *Science* **1994**, *266*, 771.
(5) Rief, M.; Oesterhelt, F.; Heymann, B.; Gau, H. E. *Science* **1997**, *275*, 1295.
(6) Treloar, L. R. G. *The physics of Rubber Elasticity*; Oxford University Press: Oxford, England, 1975.
(7) Edwards, S. F.; Vilgis, T. A. *Rep. Prog. Phys.* **1988**, *51*, 243.
(8) Doi, M.; Edwards, S. F. *The theory of polymer dynamics*; Oxford Clarendon Press: Oxford, England, 1986.
(9) Pincus, P. *Macromolecules* **1976**, *9*, 386.
(10) de Gennes, P. G. *Scaling concepts in Polymer Physics*; Cornell University Press: Ithaca, NY, 1979.
(11) Grosberg, A. Yu.; Khokhlov, A. R. *Statistical Physics of Macromolecules*; AIP: New York, 1994.
(12) Halperin, A.; Zhulina, E. B. *Eur. Phys. Lett.* **1991**, *15*, 417.
(13) Vilgis, T. A.; Johner, A.; Joanny, J.-F. *Eur. Phys. J. E* **2000**, *2*, 289.
(14) Limbach, H. J. Ph.D. Thesis. Struktur und Eigenschaften von Polyelektrolyten im schlechten Lösungsmittel. Johannes Gutenberg-Universität, Mainz, Germany, 2001.
(15) Tamashiro, M. N.; Schiessel, H. *Macromolecules* **2000**, *33*, 5263.
(16) Lai, P.-Y. *Phys. Rev. E* **1998**, *58*, 6222.
(17) Lee, N.; Vilgis, T. A. *Europhys. Lett.* **2002**, *57*, 817.
(18) Gorbunov, A.; Skvortsov, A. *J. Chem. Phys.* **1993**, *98*, 5961.
(19) More precisely, $D = |\mu|^{-\nu/\phi}$. The exponent ϕ is given by the number of monomers g interacting with surface, i.e. $g^\phi|\mu| = k_BT$.
(20) Pincus, P.; Sandroff, C. J.; Witten, Jr. T. A. *J. Phys. (Fr.)* **1984**, *45*, 725.
(21) There is a discussion about the conformation of the adsorbed loop size whether the overall loop size will be increased due to the excluded volume interactions instead of the picture we used where the remaining chain ($N > N^*$) takes random walk configurations.
(22) Johner, A.; Bouchaud, E.; Daoud, M. *J. Phys. (Fr.)* **1990**, *51*, 495.
(23) Lepine, Y.; Caille, A. *Can. J. Phys.* **1978**, *56*, 403.
(24) Eisenriegler, E.; Kremer, K.; Binder, K. *J. Chem. Phys.* **1982**, *77*, 6296.
(25) Leibler, L.; Orland, H.; Wheeler, J. C. *J. Chem. Phys.* **1983**, *79*, 3550.
(26) The usual argument is kinetic and may be somewhat weaker here as the chains are already adsorbed on one plate.

However to change the amount of B-polymer in the contact area, the surface density of A/B junction points has to be changed. To see whether this is thermodynamically favored or not requires a more detailed study of the polymer conformations in the core.
(27) Borisov, O. V.; Halperin, A. *Eur. Phys. J. B.* **1999**, *9*, 251.
(28) Ji, H.; Hone, D.; Pincus, P. A.; Rossi, G. *Macromolecules* **1990**, *23*, 698.
(29) Johner, A.; Joanny, J.-F. *Macromol. Theory Simul.* **1997**, *6*, 479.
(30) Derjaguin, B. V. *Kolloid Z.* **1934**, *69*, 155.
(31) Fleer, G. J.; Cohen-Stuart, M. A.; Scheutjens, J. M. H. M.; Cosgrove, T.; Vincent, B. *Polymers at Interfaces*; Chapman Hall: London, 1993.
(32) Jimenez, J.; de Joannis, J.; Bitsanis, I.; Rahagopalan, R. *Macromolecules* **2000**, *33*, 7157.
(33) Strictly speaking, the effect of the third virial is nonperturbative as the concentration profile becomes nonexponential (for a single plate).
(34) A more qualitaive argument is as follows. For small separations ($z < 2D$), the concentration in the gap is almost uniform and $\phi = 1/zb^2$, and the free energy comprises an adsorption contribution and a third virial contribution: $F = -Nb^2/zD + wb^{-6}/3!Nb^2/z^{2.}$ The force is dominated by the excluded volume term $\varphi = -wb^{-6}/3Nb^2/z^3$ and is repulsive.
(35) Semenov, A. N.; Joanny, J. F.; Khoklov, A. R. *Macromolecules* **1995**, *28*, 1066.
(36) Feller, W. *An Introduction to Probability Theory and its Application*; John Wiley & Sons: New York, 1957.
(37) Lee, N.; Vilgis, T. A. condmat No. 0110581.

MA012208Q